



Thermally activated magnetization back-hopping based true random number generator in nano-ring magnetic tunnel junctions

Cite as: Appl. Phys. Lett. **114**, 112401 (2019); <https://doi.org/10.1063/1.5077025>

Submitted: 24 October 2018 . Accepted: 02 March 2019 . Published Online: 18 March 2019

Jiaying Qin, Xiao Wang, Tao Qu , Caihua Wan, Li Huang, Chenyang Guo, Tian Yu, Hongxiang Wei, and Xiufeng Han 

COLLECTIONS

 This paper was selected as an Editor's Pick



View Online



Export Citation



CrossMark

Applied Physics Reviews
Now accepting original research

2017 Journal
Impact Factor:
12.894

AIP
Publishing

Thermally activated magnetization back-hopping based true random number generator in nano-ring magnetic tunnel junctions

Cite as: Appl. Phys. Lett. **114**, 112401 (2019); doi: [10.1063/1.5077025](https://doi.org/10.1063/1.5077025)

Submitted: 24 October 2018 · Accepted: 2 March 2019 ·

Published Online: 18 March 2019





View Online



Export Citation



CrossMark

Jianying Qin,¹ Xiao Wang,¹ Tao Qu,²  Caihua Wan,¹ Li Huang,¹ Chenyang Guo,¹ Tian Yu,³ Hongxiang Wei,¹ and Xiufeng Han^{1,a)} 

AFFILIATIONS

¹Beijing National Laboratory for Condensed Matter Physics, Institute of Physics, Chinese Academy of Sciences, University of Chinese Academy of Sciences, Beijing 100190, China

²School of Physics and Astronomy, University of Minnesota-Twin Cities, Minneapolis, Minnesota 55455, USA

³College of Physical Science and Technology, Sichuan University, Chengdu 610065, China

^{a)}Email: xfhan@iphy.ac.cn

ABSTRACT

A true random number generator based on the magnetization backhopping process in nano-ring magnetic tunnel junctions is demonstrated in this work. The impact of environmental temperature (T) and current pulse width (τ) on backhopping is investigated statistically by experiments, micromagnetic simulations, and theoretical analysis. The backhopping probability increases at high T and wide τ , as explained by the combined effect of thermal fluctuation and spin-transfer-torque noise. The magnetoresistance at backhopping is randomly distributed over a large operational current range. This manifestation of backhopping in magnetic tunnel junctions can be used as the basic unit of a true random number generator.

Published under license by AIP Publishing. <https://doi.org/10.1063/1.5077025>

Random numbers have been indispensably used in a wide variety of applications ranging from cryptography to statistics. Pseudo-random number generators (PRNGs)—which generate a sequence of numbers from a seed using a computer program—are often used because of their high operating rate of about 100 Gbps.¹ However, there exist severe security limitations for the PRNGs because the generated sequences can be decoded mathematically. Thus, true random number generators (TRNGs) based on physical processes with complete indeterminacy are desirable. Until now, several approaches, such as quantum optics, jitter oscillators, and physical noise source amplification,^{2–6} have been developed to generate true random numbers (RNs). In general, enhanced technological applicability would greatly benefit from CMOS compatibility, low power dissipation, and compactness. TRNGs based on the magnetization backhopping process in nano-ring shaped magnetic tunneling junctions (NR-MTJs) are promising candidates with several advantages. First, according to previous reports,^{7–13} NR-MTJs can eliminate stray fields between each other, which will lead to high areal density, further resulting in a high RN generation rate. Second, the formation of the “Onion” state for the free layer magnetization in the NR-MTJs can reduce the energy barrier of

the cell¹⁴ and eliminate the thermal turbulence on the sub-50 nm in-plane MTJs,¹⁵ both of which favoring the functioning of the TRNGs as discussed below. Besides, backhopping occurs within nanoseconds, which allows the TRNG to work near GHz frequencies. Also, no initializing operations are required before the generation of RNs. Finally, the simpler two-terminal device, high throughput,^{5,16,17} low power consumption of less than 1 fJ (Ref. 18) and theoretically infinite operating times¹⁰ of MTJs also make it a competitive candidate for TRNGs.

In MTJ devices, the backhopping phenomenon occurs mainly in the current induced magnetization reorientation^{19–22} process. At low current, spin transfer torque (STT) plays the role of a driving force that stably sets the two magnetic layers in either parallel (P) or anti-parallel (AP) states, which corresponds to low and high resistances, respectively.^{7–11,23,24} With further increase of current, the magnetization will be driven deviating from the stable state and fluctuates between P and AP states.^{15,25–32}

In this article, the characteristics of backhopping in NR-MTJs are investigated. We find that the probability of the emergence of backhopping depends on the measurement temperature T and current

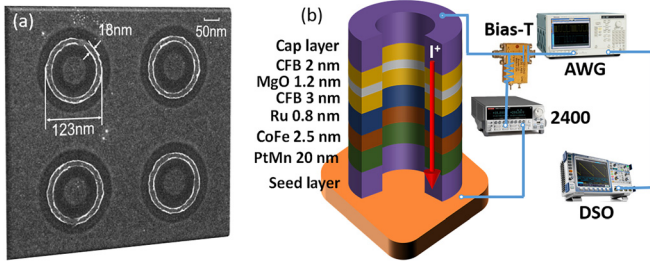


FIG. 1. (a) The SEM image of the NR-MTJs. (b) The multilayer structure and the setup of the measurement system. CFB stands for CoFeB. The current pulse comes from the arbitrary waveform generator (AWG) and is monitored with a digital storage oscilloscope (DSO). The resistance is measured with a Keithley 2400 voltage meter.

pulse width τ . The distribution of resistance in the backhopping current range is totally random, which is taken as the basis of the TRNG. All the experimental results are reproduced well by micromagnetic simulations, which also explains the mechanism of backhopping from the perspective of energy.

The experiments are performed in two hundred NR-MTJ devices. The ring shape is fabricated using electron beam lithography and has inner and outer radii of 40 nm and 60 nm, respectively, as shown in Fig. 1(a). The stack structure is depicted in Fig. 1(b), with the free layer and the reference layer being in-plane magnetized (more information is included in supplementary material Fig. S1). The measurement setup is shown in Fig. 1(b). A square wave current pulse is injected into the MTJ device through a bias-tee to switch the magnetization of the free layer. Resistance measurements are performed after the pulse ends via the inductance terminal. All these measurements are done in zero magnetic field.

Figure 2(a) shows the current manipulated magnetization switching process, which can be divided into three regions: (I) a normal STT switching hysteresis loop with the critical switching current I_{cs} and (II and III) two backhopping regions^{22,25,32} with the starting current I_{bh} . Backhopping occurs when the current amplitude is above I_{bh} . Actually, 200 NR-MTJs are measured, but not all of them are observed with backhopping. We consider the probability of backhopping P_{bh} (the amount of backhopping MTJs out of the 200 ones) as functions of T and τ . The details of the measurement method are discussed in the supplementary material, Part V. For example, in Fig. 2(b), for a relatively short pulse, such as 10 ns, backhopping occurs in 22% of the devices at room temperature. As τ increases to 1 μ s, P_{bh} is enhanced to 82% and then saturates at 92% when τ reaches 1 ms. On the other hand, T also impacts the behavior of backhopping, as revealed by Fig. 2(c). More than 75% of MTJs stay in the stable P state at low T (below

150 K) and short τ (shorter than 100 ns), in which case the backhopping does not happen. Then, a quick increase in P_{bh} occurs when T and τ increase, until the percentage reaches 90% for τ longer than 100 μ s and T above 220 K. For devices operating at room temperature, a short pulse of $\tau = 10$ ns can drive more than 20% of the NR-MTJs into backhopping, which means that backhopping can be triggered at ~ 100 MHz.

It is also noticed that an asymmetry for P to AP and AP to P backhopping exists in Fig. 2(b), and the former circumstance shows a higher probability than the latter one. This is related to the current shift in positive and negative directions in regions I and II shown in Fig. 2(a), where $-I_{bh} = -580 \mu$ A, while $I_{bh} = 480 \mu$ A. This may be a result of the asymmetric influence on bias behavior of spin torque,³³ and the deviation from an ideal ring shape inadvertently introduced during experimental fabrication. It can be compensated by reducing the current amplitude by -70μ A for P to AP transition (positive current direction) shown by the cyan triangles in Fig. 2(b), where the two probabilities overlap well with each other. Besides, multiplied by the resistance of the AP state, which is around 1250 Ω , the backhopping voltage is about 750 mV. This value is quite smaller than the report of Min. *et al.*²² This can be attributed to the ring shape design, which can result in lower critical current due to the “onion” magnetization state.¹⁴

Previous research works have reported that backhopping occurs because of thermal activated magnetization perturbation,^{15,22,27,31} which originates similarly to the thermally assisted magnetization switching process. Min *et al.*²² describe this mechanism as follows:

$$I_{cs,bh} = I_{cs0,bh0} \left[1 - \frac{k_B T}{E_{cs,bh}} \ln \left(\frac{\tau}{\tau_0} \right) \right], \quad (1)$$

where k_B is the Boltzmann constant, $E_{cs,bh}$ is the energy barrier of the critical switching or backhopping, $I_{cs0,bh0}$ characterizes the $I_{cs,bh}$ at 0 K, respectively, and $1/\tau_0$ is the attempt frequency. I_{bh} follows the same rule of evolution as I_{cs} that larger critical current is needed to trigger backhopping at low T and shorter τ . This is consistent with the observation shown in Figs. 3(a) and 3(b) that $I_{cs,bh}$ depends on T and $\ln(\tau/\tau_0)$ linearly and monotonically. There always exists a gap between I_{bh} and I_{cs} , which means that the barrier of backhopping is larger than that of current induced magnetization switching. Accordingly, at room temperature, E_{bh} is estimated to be about $1.62E_{cs}$, while the thermal stability, depicted by $\Lambda = \frac{E_{bh}}{k_B T}$, is derived to be about 56 and inversely proportional to T shown in Fig. 3(a). Actually, this value is relatively low compared to Λ obtained in most of the MgO based MTJs in previous reports,^{34,35} which directly leads to the instability of magnetization that can be excited into backhopping.

The magnetization switching rate $\gamma_{1,2}$ (for AP to P and P to AP, respectively) can be expressed as a function of I_{bh} ^{31,32} as follows:

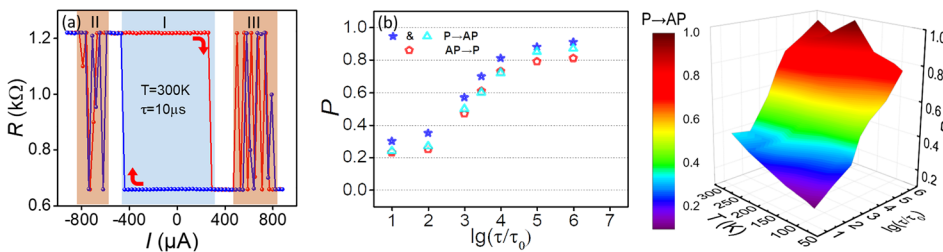


FIG. 2. (a) Current with τ of 1 μ s induced magnetization switching at RT in NR-MTJs. (b) P_{bh} for different τ at room temperature in both positive and negative current. (c) The contour map of P_{bh} vs T and τ . Here, just the positive pulse current driven switching is taken into consideration.

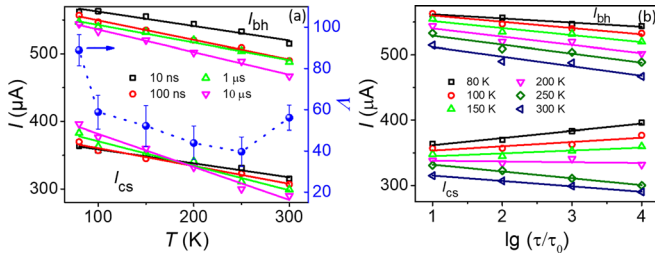


FIG. 3. (a) and (b) T and τ dependence of I_{cs} , I_{bh} , and Λ .

$$\gamma_{1,2} = \gamma_0 \exp \left[-\frac{C}{k_B T} (H_K \mp H_{eff})^2 \left(1 \mp \frac{I_{bh}}{I_{bh0}} \right) \right], \quad (2)$$

where H_{eff} is the effective field which includes the contribution of magnetocrystalline anisotropy and stray field, C is a constant in the energy scale, H_K is the free layer shape anisotropy (should be 0 in the NR-MTJs), and γ_0 denotes the attempt frequency

$$P_{1,2}(\tau) \sim \frac{\gamma_{1,2}}{\gamma_1 + \gamma_2} \{ 1 - \exp[-(\gamma_1 + \gamma_2)\tau] \}. \quad (3)$$

Considering that the parameters in Eq. (2) vary much slower than the magnetization switching time in sub-nanoseconds, the switching probability as functions of $\gamma_{1,2}$ and τ can be derived into Eq. (3), where $P_{1,2}$ is the probability of magnetization in P and AP states, respectively.³² P_2 stands for P_{bh} the positive current, the magnetization switching from the P state back to the AP state means the backhopping happens. By comparing P_1 and P_2 as shown in Eq. (4), where $A = \frac{2CH_{eff}^2}{k_B}$ and $B = \frac{2CH_{eff}^2}{E_{bh}}$, it is clear that backhopping happens at higher temperatures and longer current pulses with a larger probability, which is consistent with the experimental results

$$\frac{P_2}{P_1} \sim \exp \left[-A \frac{1}{T} + B \ln \left(\frac{\tau}{\tau_0} \right) \right]. \quad (4)$$

In the following, the distribution of the resistance in the backhopping region is explored. In Fig. 2(a), $I_{bh} = 480 \mu A$ in region III. Thus, we select the pulse current with the amplitude of $640 \mu A$ (larger than I_{bh}) and τ of 10 ns at room temperature to inject into the NR-MTJs, which can ensure the occurrence of backhopping by larger probability. After the current pulse, a relaxation time of 1 s is adopted, which is long enough for the relaxation of the heating generated by current. Then, the resistance is read out by a low current with the amplitude of 100 nA, which would not disturb the tested resistance state. The results of 20 000 testing cycles are summarized in Fig. 4(a) (only 200 results are plotted here for clear visibility), which shows no obvious regularity of the resistance distribution visually. It is found that the resistances are mainly distributed in the P or AP state, with a few intermediate values. By applying a reference sorter $(R_{max} + R_{min})/2$, which classifies resistance values larger than the reference as 1 and otherwise as 0, a sequence of pure 0 and 1 is obtained as a mosaic pattern in Fig. 4(b). A $\pm 40 \mu A$ deviation of trigger current does not affect the results, indicating the stability of the devices [shown in Fig. 4(b) and supplementary material Figs. S3(e) and S3(f)]. Then, the reliability of randomness of the number sequence (20 000 numbers) is examined according to the randomness testing suites of FIPS 140-1 and STS 2.1.1, issued by

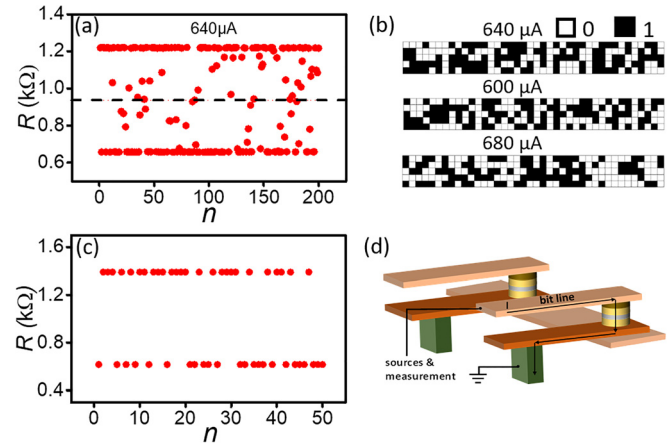


FIG. 4. (a) Distribution of the resistance in the backhopping region under a bias current of $640 \mu A$. The reference level is represented by the black dashed line. (b) Distribution of the logic values under different bias currents. The arrow represents the direction of the zigzag arrangement of the 200 logic values. (c) Distribution of 50 consecutive resistances obtained by micromagnetic simulation. (d) Schematic diagram of a TRNG device employing an array of NR-MTJs.

the National Institute of Standards and Technology (NIST).^{5,36-39} The results of both suites show that all the tests have been passed (see supplementary material, Table S1 and Fig. S2), indicating high quality of the randomness for the number sequence.

In order to gain an insight into the backhopping state, micromagnetic simulations based on the Landau-Lifshitz-Gilbert (LLG) equation,^{40,41} as shown in the following equation, are performed:

$$\frac{d\hat{m}}{dt} = -\gamma \hat{m} \times (\vec{H}_{eff} + \vec{\eta}) + \alpha \hat{m} \times \frac{d\hat{m}}{dt} + a_1 \hat{m} \times (\hat{m} \times \hat{m}_p) + b_1 (\hat{m} \times \hat{m}_p), \quad (5)$$

where γ , α , and \hat{m} are the gyromagnetic ratio, the damping constant, and the unit vector of local magnetization in the free layer, respectively. Assuming that the reference layer is solidly pinned by the synthetic anti-ferromagnetic layer of PtMn as shown in the $M-H$ loop in supplementary material S1, the interlayer coupling from the reference layer acts as a constant bias field and cannot contribute much to backhopping. Thus, we mainly focus on the impact of thermal fluctuation and the STT effect on the free layer magnetization operation.^{25,26,28,32}

In LLG Eq. (5), $\vec{\eta}$ is the thermal fluctuation field,^{42,43} described by a white noise with an amplitude dependent on temperature. In addition, two STT terms: current induced in-plane Slonczewski torque a_1 ¹⁹ and field-like torque b_1 ^{44,45} are implemented in the LLG equation. The factors a_1 is equal to $\frac{\hbar \gamma P J}{2e M_s d}$ and b_1 is $e V^2$, where e is the magnitude of the electron charge, P is the polarization constant, J is the current density, M_s is the free layer saturation magnetization and d is the thickness of the free layer. In the micromagnetic simulation, the following parameters are used for the free layer: the thickness is 2 nm, $M_s = 774 \text{ emu/cm}^3$, the exchange constant $A = 1.0 \times 10^{-6} \text{ erg/cm}$, the perpendicular uniaxial anisotropy $K_{\perp} = 2.79 \times 10^6 \text{ erg/cm}^3$, the in-plane anisotropy $K_{\parallel} = 3.87 \times 10^4 \text{ erg/cm}^3$, $P = 0.2$ and $\alpha = 0.024$. These parameters are derived from micromagnetic simulation fitting to the $M-H$ loop and I_{cs} . τ is set to 10 ns. The current amplitude is

increased by 30 μA steps to 900 μA , until backhopping occurs. The simulated Curie temperature from these parameters is 700 K, which is substantially above the device working temperature.

Figure 5(a) shows the simulated current driven magnetization switching results. We can also see three regions, including backhopping, where I_{cs} and I_{bh} are equal to 270 μA and 480 μA , respectively, just as depicted by Fig. 2(a). To demonstrate the mechanism of backhopping, the magnetization motion related to the system energy evolution is simulated as well, as shown in Figs. 5(b) and 5(c). We can see that when the current increases to 270 μA , the increment of system energy resulting from the enlarging in-plane STT reaches the extreme value at 2 ns, which is sufficient to overcome the damping torque and achieve the magnetization switching from the $-x$ direction to the $+x$ one. After the current is off, the injected energy from the STT quickly dissipates due to the damping effect, and the system relaxes to the low energy state. Then, with current enlarged to 360 μA , the energy also keeps increasing. The magnetization tends to switch away from the $+x$ direction at the beginning of 8 ns. But, this high energy state is not sufficient to overcome the energy barrier of backhopping. Thus, it returns to the P state after the pulse is off. As a result, backhopping does not happen. However, when the current reaches 480 μA , the system energy reaches a maximum at 10 ns and the magnetization finally switches back to the $-x$ direction again. In previous research,²⁹ it is reported that the quadratic dependence of field-like torque on the applied voltage leads to a steady precession of magnetization during the current pulse and backhopping is measured when the pulse ends. However, in our simulation, once the contribution of thermal fluctuation is removed, backhopping does not happen for any current up to 900 μA . In fact, the estimated field-like torque is about 10 Oe in the $+x$ direction and is negligible compared to the thermal fluctuation

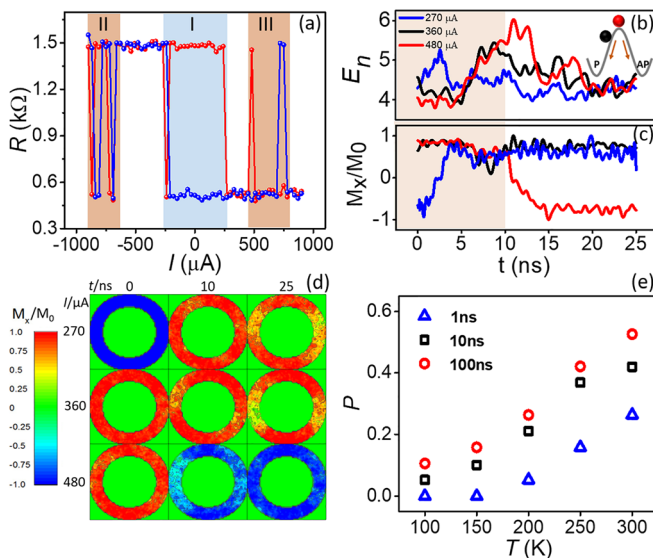


FIG. 5. (a) The simulated current switching magnetization results of the NR-MTJ at room temperature with a τ of 10 ns. (b) and (c) The time evolution of the total energy and the component of magnetization in the x direction for 270 μA , 360 μA , and 480 μA with τ of 10 ns. (d) The magnetization and the domain motion under different currents in NR-MTJs. (e) P_{bh} calculated from multiple scans versus T and τ by micromagnetic simulations.

noise, whose amplitude is around 38 000 Oe in this simulation.⁴² Thus, we can say that backhopping is caused by a combined effect of in-plane STT and thermal fluctuation. Both of these two factors can introduce noise into the magnetic system. Thus, at this point, both STT and the thermal effect stimulate the system to a maximum energy state, as shown in Fig. 5(b). Then, the system has equal possibility to fall into the low energy state of P or AP, as shown in the inset of Fig. 5(b). The corresponding domain evolution under the processes mentioned above is summarized in Fig. 5(d): the current of 270 μA provides sufficient STT to switch the magnetization from the initial $-x$ direction to the $+x$ one; the current of 360 μA cannot switch the magnetization back to the $-x$ direction due to the high backhopping barrier; the current of 480 μA finally triggers the backhopping by switching the magnetization back to the $-x$ direction. The resistance distribution at 600 μA (in Region III) within 50 cycles is also simulated and depicted in Fig. 4(c), in which the states of P and AP are purely randomly chosen with no preference and the self-correlation of the resistance state is 0, indicating a high quality random number sequence.

Finally, the T and τ dependence of P_{bh} is also simulated. At a low T of 100 K, shown in Fig. 5(e), even with τ of 100 ns, less than 12% of all the devices show backhopping behavior. For τ less than 1 ns, backhopping is not present at all. P_{bh} increases remarkably with increasing T , as well as for longer τ . For a τ of 100 ns at 300 K, approximately 52% of the scans show backhopping. Although other simulations with longer τ were not conducted owing to excessive computational cost, the effects of T and τ on backhopping can now semi-quantitatively reproduce the experimental results. It should be noticed that at room temperature, experimentally, 10 ns-pulse-width current can trigger a P_{bh} of 22%, while theoretically, this percentage is 20% for $\tau = 1$ ns. Besides, analogous to MRAM, if a series of N NR-MTJs are arranged in parallel connection as shown in Fig. 4(d), in general, a random number sequence containing 2^N numbers can be obtained. Thus, the TRNG generating rate can be as high as ~ 100 MHz, even ~ 1 GHz with an infinite sequence length, which can cover most applications. It is not easy to forwardly improve the functioning frequency because the magnetization switching duration is around the nanosecond scale.^{46,47} But, still some investigations reported that by optimizing the structure of the MTJs, the functioning time can be reduced to the femtosecond scale,⁴⁸ which sheds light on the application of the NR-MTJs based TRNGs at higher frequencies.

In summary, backhopping is observed in nano-ring MTJ devices. We find that backhopping occurs more frequently at high T and wide τ . The resistance in the backhopping region appears to follow a truly random distribution. Micromagnetic simulations show that backhopping is stimulated by the combination of in-plane STT and thermal noise. The ability of backhopping to rapidly generate a sequence of random resistances suggests feasibility for a high quality TRNG that can work at up to gigahertz frequency generation rate.

See [supplementary material](#) for a summary of the M - H loop of the film, the details of the randomness reliability of the number sequences by the suites of NIST, the device lifetime exploration, the breakdown of the devices, and the method of determining P_{bh} .

This work was supported by the National Key Research and Development Program of China (MOST, Grant No. 2017YFA0206200) and

the National Natural Science Foundation of China (NSFC, Grant Nos. 11434014, 51620105004, and 11674373) and partially supported by the Strategic Priority Research Program (B) (Grant No. XDB07030200), the International Partnership Program (Grant No. 112111KYSB20170090), and the Key Research Program of Frontier Sciences (Grant No. QYZDJ-SSWSLH016) of the Chinese Academy of Sciences (CAS). This work was also supported by the University of Minnesota Supercomputing Institute for computer time.

REFERENCES

- ¹Y. Bouvier, M. Nagatani, H. Nosaka, K. Kurishima, N. Kashio, M. Ida, and K. Murata, in *IMS* (IEEE, 2014), p. 1109.
- ²B. Sanguinetti, A. Martin, H. Zbinden, and N. Gisin, *Phys. Rev. X* **4**, 031056 (2014).
- ³M. W. Mitchell, C. Abellan, and W. Amaya, *Phys. Rev. A* **91**, 012314 (2015).
- ⁴Z. Cao, H. Zhou, X. Yuan, and X. Ma, *Phys. Rev. X* **6**, 011020 (2016).
- ⁵W. H. Choi, Y. Lv, J. Kim, A. Deshpande, G. Kang, J.-P. Wang, and C. H. Kim, in 2014 IEEE IEDM (2014).
- ⁶Y. Kim, X. Fong, and K. Roy, *IEEE Magn. Lett.* **6**, 3001004 (2015).
- ⁷Z. Li, H. Zhang, L. Wang, G. Wu, H. Wu, X. Bi, H. H. Li, Y. Chen, J. Qin, P. Guo, W. Kong, W. Zhan, and X. Han, in *ISLPED 2016* (ACM, 2016).
- ⁸X. F. Han, Z. C. Wen, Y. Wang, H. F. Liu, H. X. Wei, and D. P. Liu, *IEEE Trans. Magn.* **47**, 2957 (2011).
- ⁹X. F. Han, Z. C. Wen, and H. X. Wei, *J. Appl. Phys.* **103**, 07E933 (2008).
- ¹⁰X. Han, Z. Wen, Y. Wang, L. Wang, H. Wei *et al.*, *AAPPS Bull.* **18**, 25 (2008).
- ¹¹T. Min, Q. Chen, R. Beach, G. Jan, C. Horng, W. Kula, T. Torng, R. Tong, T. Zhong, D. Tang *et al.*, *IEEE Trans. Magn.* **46**, 2322 (2010).
- ¹²H.-X. Wei, M. C. Hickey, G. I. R. Anderson, X.-F. Han, and C. H. Marrows, *Phys. Rev. B* **77**, 132401 (2008).
- ¹³H.-X. Wei, J. He, Z.-C. Wen, X.-F. Han, W.-S. Zhan, and S. Zhang, *Phys. Rev. B* **77**, 134432 (2008).
- ¹⁴H. Liu, H. Wei, X. Han, G. Yu, W. Zhan, S. Le Gall, Y. Lu, M. Hehn, S. Mangin, M. Sun *et al.*, *Phys. Rev. Appl.* **10**, 054013 (2018).
- ¹⁵V. Korenivski and R. Leuschner, *IEEE Trans. Magn.* **46**, 2101 (2010).
- ¹⁶A. Fukushima, T. Seki, K. Yakushiji, H. Kubota, H. Imamura, S. Yuasa, and K. Ando, *Appl. Phys. Exp.* **7**, 083001 (2014).
- ¹⁷H. Lee, F. Ebrahimi, P. K. Amiri, and K. L. Wang, *AIP Adv.* **7**, 055934 (2017).
- ¹⁸R. Dorrance, J. G. Alzate, S. S. Cherepov, P. Upadhyaya, I. N. Krivorotov, J. A. Katine, J. Langer, K. L. Wang, P. K. Amiri, and D. Markovic, *IEEE Electron Device Lett.* **34**, 753 (2013).
- ¹⁹J. Slonczewski, *J. Magn. Magn. Mater.* **159**, L1 (1996).
- ²⁰L. Berger, *Phys. Rev. B* **54**, 9353 (1996).
- ²¹J. A. Katine, F. J. Albert, R. A. Buhrman, E. B. Myers, and D. C. Ralph, *Phys. Rev. Lett.* **84**, 3149 (2000).
- ²²T. Min, J. Z. Sun, R. Beach, D. Tang, and P. Wang, *J. Appl. Phys.* **105**, 07D126 (2009).
- ²³B. Engel, J. Akerman, B. Butcher, R. Dave, M. DeHerrera, M. Durlam, G. Grynckewich, J. Janesky, S. Pietambaram, N. Rizzo *et al.*, *IEEE Trans. Magn.* **41**, 132 (2005).
- ²⁴B. Tao, H. Yang, Y. Zuo, X. Devaux, G. Lengaigne, M. Hehn, D. Lacour, S. Andrieu, M. Chshiev, T. Hauet *et al.*, *Phys. Rev. Lett.* **115**, 157204 (2015).
- ²⁵S.-C. Oh, S.-Y. Park, A. Manchon, M. Chshiev, J.-H. Han, H.-W. Lee, J.-E. Lee, K.-T. Nam, Y. Jo, Y.-C. Kong *et al.*, *Nat. Phys.* **5**, 898 (2009).
- ²⁶Z. Hou, Y. Liu, S. Cardoso, P. P. Freitas, H. Chen, and C.-R. Chang, *J. Appl. Phys.* **109**, 113914 (2011).
- ²⁷J. Heinen, D. Hinzke, O. Boulle, G. Malinowski, H. J. M. Swagten, B. Koopmans, C. Ulysse, G. Faini, and M. Kläui, *Appl. Phys. Lett.* **99**, 242501 (2011).
- ²⁸W. Kim, S. Couet, J. Swerts, T. Lin, Y. Tomczak, L. Souriau, D. Tsvetanova, K. Sankaran, G. L. Donadio, D. Crotti *et al.*, *IEEE Trans. Magn.* **52**, 3401004 (2016).
- ²⁹K. Bernert, V. Sluka, C. Fowley, J. Lindner, J. Fassbender, and A. M. Deac, *Phys. Rev. B* **89**, 134415 (2014).
- ³⁰S. Manipatruni, D. E. Nikonov, and I. A. Young, *J. Appl. Phys.* **115**, 17B754 (2014).
- ³¹N. D. Rizzo, M. DeHerrera, J. Janesky, B. Engel, J. Slaughter, and S. Tehrani, *Appl. Phys. Lett.* **80**, 2335 (2002).
- ³²J. Z. Sun, M. C. Gaidis, G. Hu, E. J. O'Sullivan, S. L. Brown, J. J. Nowak, P. L. Trouilloud, and D. C. Worledge, *J. Appl. Phys.* **105**, 07D109 (2009).
- ³³Y.-H. Tang, N. Kioussis, A. Kalitsov, W. Butler, and R. Car, *Phys. Rev. B* **81**, 054437 (2010).
- ³⁴P. Upadhyaya, P. K. Amiri, A. A. Kovalev, Y. Tserkovnyak, G. Rowlands, Z. Zeng, I. Krivorotov, H. Jiang, and K. L. Wang, *J. Appl. Phys.* **109**, 07C708 (2011).
- ³⁵D. Mazumdar, X. Liu, B. Schrag, W. Shen, M. Carter, and G. Xiao, *J. Appl. Phys.* **101**, 09B502 (2007).
- ³⁶J. Soto, <http://csrc.nist.gov/nissc/1999/proceeding/papers/p24.pdf> for "Statistical testing of random number generators" (1999).
- ³⁷M. Ren, E. Wu, Y. Liang, Y. Jian, G. Wu, and H. Zeng, *Phys. Rev. A* **83**, 023820 (2011).
- ³⁸D. Ankur and V. Pareek, in *IJCA Proceedings of the International Conference on Advances in Computer Engineering and Applications, ICACEA(2)* (IICA, 2014), pp. 19–28.
- ³⁹F. Sun and S. Liu, *Chaos, Solitons Fractals* **41**, 2216 (2009).
- ⁴⁰Y.-H. Tang, N. Kioussis, A. Kalitsov, W. H. Butler, and R. Car, *J. Phys.: Conf. Ser.* **200**, 062033 (2010).
- ⁴¹N. A. Natekar, W.-H. Hsu, and R. H. Victora, *AIP Adv.* **7**, 056004 (2017).
- ⁴²W. F. Brown, *Phys. Rev.* **130**, 1677 (1963).
- ⁴³Z. Liu, P.-W. Huang, G. Ju, and R. H. Victora, *Appl. Phys. Lett.* **110**, 182405 (2017).
- ⁴⁴K. Xia, P. J. Kelly, G. E. W. Bauer, A. Brataas, and I. Turek, *Phys. Rev. B* **65**, 220401 (2002).
- ⁴⁵I. Theodonis, N. Kioussis, A. Kalitsov, M. Chshiev, and W. H. Butler, *Phys. Rev. Lett.* **97**, 237205 (2006).
- ⁴⁶R. Koch, J. Katine, and J. Sun, *Phys. Rev. Lett.* **92**, 088302 (2004).
- ⁴⁷T. Devolder, J. Hayakawa, K. Ito, H. Takahashi, S. Ikeda, P. Crozat, N. Zerounian, J.-V. Kim, C. Chappert, and H. Ohno, *Phys. Rev. Lett.* **100**, 057206 (2008).
- ⁴⁸H. Liu, D. Bedau, D. Backes, J. Katine, J. Langer, and A. Kent, *Appl. Phys. Lett.* **97**, 242510 (2010).